

UNSTEADY DRAG ON SUBMERGED STRUCTURES

F. J. Moody

ABSTRACT

Drag forces occurring on submerged structures in a pressure suppression pool during air expulsion and air bubble oscillation are examined in this study. The total force on a structure is composed of an acceleration drag component, caused by the unsteady flow, and a standard drag component associated with the instantaneous velocity field. Formulas are given for estimating the acceleration drag on common submerged structures.

B604020099 860114
PDR FOIA
FIREST085-665 PDR

INTRODUCTION

Whenever air is discharged into a pressure suppression pool, forces created on submerged structures by pool water motion must be considered in the mechanical design. If the disturbance causing water motion is rapid compared to sonic transit time in the pool, acoustic loads of brief duration will be generated. Acoustic loads on submerged structures usually involve small impulses, and are not considered in the present work. This study is devoted to loads caused by unsteady bulk pool water motion.

Steady flow forces on submerged objects usually are predicted with the help of standard drag coefficients, which include effects of both dynamic pressure and skin friction. Dynamic pressure drag is caused by fluid velocity impingement on the submerged object, which raises pressure on the side toward oncoming flow, and lowers pressure on the other side due to wake formation. Skin friction drag is caused by viscous shear stress on the lengthwise surface of the submerged object.

Standard drag coefficients for submerged objects usually are based on steady state uniform flow without pressure gradients in the flowing stream. However, time-dependent pressure gradients associated with unsteady flows result in

an additional force to be included in the design of submerged structures.

The purposes of this study are: (1) to determine the unsteady nature of both acceleration and standard drag forces caused by unsteady submerged air discharge or bubble oscillation in a suppression pool; and (2) to provide a method for estimating the acceleration drag on various submerged structural elements.

SUMMARY AND CONCLUSIONS

Air discharge into a suppression pool from either a postulated loss of coolant accident or a relief valve blow will impose forces on submerged structures due to unsteady bulk fluid motion. Fluid acceleration imposes acceleration drag forces, and fluid velocity imposes both dynamic pressure and skin friction drag forces which, when combined, are referred to as either standard or steady drag.

A submerged gas volume may be in the process of charging, e.g., during drywell blowdown into the pool associated with a loss of coolant accident, or during relief valve expulsion of initial pipe air, or a submerged gas bubble may be oscillating after it has been charged. For either charging or oscillating, an idealized spherical gas bubble is employed to produce a radially symmetric flow field. For a submerged

structure at some radius from the bubble center, the flow field in a neighborhood about the structure is approximated by uniform flow, whose velocity and acceleration correspond to the generating bubble motion. Total drag on a submerged structure should be estimated as the sum of standard and acceleration drag components, F_{STAN} and F_{ACCEL} . The standard drag force is obtained in the usual way from

$$F_{STAN} = C_D A \frac{U_\infty^2}{2g_c} \rho \quad (Eq. 10)$$

where ρ is surrounding fluid density, C_D is a combined pressure and skin friction drag coefficient obtained from standard tables or graphs for the particular geometry, A is the structure area projected on a plane normal to the flow field direction, and U_∞ is the equivalent uniform flow velocity, determined from

$$U_\infty = \dot{R} \left(\frac{R}{r} \right)^2$$

\dot{R} = bubble wall velocity

R = bubble radius

r = distance from bubble center to structure

For a charging bubble at pressure P_0 and undisturbed pool pressure P_∞ ,

$$\left. \begin{aligned} \dot{R}^2 &\leq \frac{2}{3} \frac{g_c}{\rho} (P_0 - P_\infty) && (Eq. 23) \\ R &\leq R_0 + \dot{R} t && (Eq. 29) \end{aligned} \right\} \text{CHARGING}$$

For an oscillating bubble, \dot{R} and R are obtained from an independent solution to the Raleigh equation,

$$\ddot{R} + \frac{3}{2} \dot{R}^2 = \frac{q_c}{\rho} (P_B - P_\infty) \quad (\text{Eq. 9})$$

where P_B is the bubble pressure corresponding to isentropic expansion and compression.

The acceleration drag, which is the main outcome of this study, is estimated from equations given in Table 1 for several common structures. The acceleration of an equivalent uniform flow field, \dot{U}_∞ , is expressed in terms of bubble radius R , wall velocity \dot{R} , and wall acceleration \ddot{R} , and distance r as

$$\dot{U}_\infty = \ddot{R} \left(\frac{R}{r} \right)^2 + \frac{2}{r^2} R \dot{R}^2 \quad (\text{Eq. 7})$$

For a charging bubble, $\ddot{R} \approx 0$. Otherwise, \ddot{R} , \dot{R} , and R are obtained from Eqs. (9), (23), and (29). The maximum acceleration drag corresponds to maximum pressure gradient in the unsteady flow field. For an oscillating bubble, maximum acceleration drag occurs when the bubble wall is at either its maximum or minimum radius, for which \dot{U}_∞ is determined

The maximum velocity is determined from the acceleration at the time of Pmax

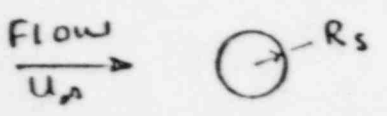
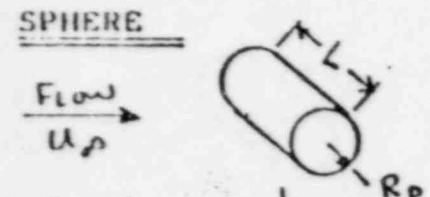
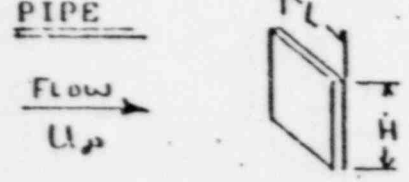
from

$$\dot{U}_\infty \text{ MAX} = \frac{1}{r^2} \frac{q_c}{\rho} \left\{ \begin{array}{l} R_{\text{MIN}} (P_{B\text{MAX}} - P_\infty) \\ R_{\text{MAX}} (P_{B\text{MIN}} - P_\infty) \end{array} \right\} \quad (\text{Eq. 31})$$

OSCILLATING

in which the product in braces is chosen which has the largest absolute value. For a charging bubble,

TABLE 1 ACCELERATION DRAG FORCE FOR SUBMERGED STRUCTURES

<u>STRUCTURE GEOMETRY</u>	<u>FORMULA</u>	<u>EQUATION IN TEXT</u>
<p>Flow U_p </p> <p><u>SPHERE</u></p>	$F = \frac{3}{2} \left(\frac{4}{3} \pi R_s^3 \right) \frac{\rho}{g_c} \dot{U}_p$	(39)
<p>Flow U_p </p> <p><u>PIPE</u></p>	$F = 2 (\pi R_p^2 L) \frac{\rho}{g_c} \dot{U}_p$	(43)
<p>Flow U_p </p> <p><u>PLATE (NORMAL TO FLOW)</u></p>	$F = \frac{1}{4} (\pi H^2 L) \frac{\rho}{g_c} \dot{U}_p$	(47)
<p>Flow U_p </p> <p><u>ANGLE (ANY ORIENTATION)</u></p>	$F < 2 (\pi R_A^2 L) \frac{\rho}{g_c} \dot{U}_p$	(50)
<p>Flow U_p </p> <p><u>I-BEAM (ANY ORIENTATION)</u></p>	$F < 2 (\pi R_I^2 L) \frac{\rho}{g_c} \dot{U}_p$	(43)

$$\dot{u}_{\infty \text{ MAX}} = \frac{R}{r^2} \frac{A}{3} \frac{g_c}{g} (P_0 - P_{\infty}) \quad \text{CHARGING (Eq. 32)}$$

where bubble radius R is estimated from Eq. (29). In the last two equations, subscripts MIN and MAX refer to minimum and maximum values of either bubble radius or pressure during oscillation, P_0 is pressure in a charging bubble, P_{∞} is undisturbed pool pressure, and t is time.

Calculated acceleration drag forces based on equivalent uniform flow fields are expected to be valid for the following constraints, imposed on bubble radius, structure characteristic dimension, and distance from the bubble center to the structure:

$$\left\{ \frac{R}{r} < 1 \quad ; \quad \frac{Z}{r} < 1 \quad , \quad Z = R_s, R_p, H, R_A, R_I \quad (\text{Eq. 57}) \right.$$

$$\text{SPHERE} \quad \frac{R_s R}{r^2} \leq \frac{2}{3} \frac{1}{C} \quad (\text{Eq. 54}) \quad ; \quad \text{PLATE} \quad \frac{H R}{r^2} \leq \frac{2}{C} \quad (\text{Eq. 56})$$

$$\text{PIPE, ANGLE, I-BEAM} \quad \frac{\sqrt{2} R}{r^2} \leq \frac{1}{2C} \quad (\text{Eq. 55})$$

where C is 1.0 for an oscillating bubble, and 4/3 for a charging bubble.

Example calculations were made for both a charging bubble and an oscillating bubble. It was found that for charging, acceleration and standard drag forces both increase as the bubble grows. This implies that maximum bubble radius should be employed in calculating design values of drag. Moreover, for an oscillating bubble it was found that the maximum drag force was equal to the maximum acceleration drag which occurred at bubble minimum radius and maximum pressure.

THE FLOW FIELD

The environment of submerged structures normally is a stagnant pressure suppression pool in which liquid velocity and pressure gradients are negligible. One form of disturbance occurs whenever a relief valve blow compresses air in the relief line and discharges it into the suppression pool where it then resembles a sphere undergoing periodic expansion and contraction until buoyancy forces it to the pool surface. Another form of disturbance would be caused by a postulated loss of coolant accident (LOCA) in which drywell air is compressed and discharged through downcomers or vent ports into the suppression pool where it expands and causes pool swell, finally breaking through the rising pool surface.

Either relief valve blow or a LOCA results in approximately spherical air volumes in the pool, which produce motion of the surrounding liquid. The associated velocity, acceleration, and pressure fields must be determined in order to predict loads on nearby submerged structures.

The bulk flow field (negligible acoustic effects) produced in liquid by motion of a submerged boundary, such as an expanding or contracting gas bubble, is governed by mass and momentum laws, written as

$$\text{MASS} \quad \nabla \cdot \vec{V} = 0 \quad (1)$$

$$\text{MOMENTUM} \quad \left(\frac{\partial}{\partial t} + \vec{V} \cdot \nabla \right) \vec{V} + \frac{\rho_0}{\rho} \nabla P = 0 \quad (2)$$

boundary layers and wakes or regions of boundary layer separation effects in the neighborhood of submerged structures are relatively small compared to the pool size. Therefore, the bulk flow field may be determined by potential flow methods, and associated loads on structures will correspond to bulk flow or free stream properties. Specifically, bulk flow solutions for various submerged geometries will provide both stream velocities to obtain viscous forces, and stream pressure gradients to determine acceleration forces.

The advantage of potential flow methods is that properties of flow fields for a number of common geometries submerged in liquid are readily obtained. However, some of the desirable potential flow patterns are based on structures submerged in uniform flow fields. In order to use these flow patterns for submerged bubble loads, first it is necessary to determine if the flow field produced by a spherical gas bubble can be treated as a uniform flow in the neighborhood of certain submerged structures.

A solution to Eq. (1) for the symmetric velocity field produced by a spherical gas bubble of radius R with wall velocity $\dot{R}(t)$ is given by

$$V_B(r, t) = \dot{R}(t)^2 \left(\frac{R(t)}{r} \right)^2 \quad (3)$$

where r is the radial distance from the sphere center to some point in the liquid. The velocity field of Eq. (3) differs noticeably from that of a uniform flow, which is

$$V_{UF}(t) = U_\infty(t) \quad (4)$$

However, the change in velocity between radii r and $r + \Delta r$ caused by a gas bubble is obtained from Eq. (3) in the form,

$$\Delta V_B(r, t) \approx -2 \frac{\dot{R}(t) R(t)^2}{r^3} \Delta r \quad (5)$$

If a length Δr is chosen so that $\frac{\Delta r}{r^3} \rightarrow 0$, it follows that the change in velocity also is small, or $\Delta V_B(r, t) \rightarrow 0$. Therefore, the flow field around a submerged structure whose dimension Δr is small relative to the cube of its distance from the bubble center is approximately one of uniform flow, whose local velocity is

$$u_p(t) \approx V_B(r, t) = \dot{R}(t) \left(\frac{R(t)}{r} \right)^2 \quad (6)$$

with local acceleration given by

$$\dot{u}_p(t) = \dot{V}_B(r, t) = \ddot{R}(t) \left(\frac{R(t)}{r} \right)^2 + \frac{2}{r^2} R(t) \dot{R}(t)^2 \quad (7)$$

Gas bubble motion is required before flow field properties can be determined from Eqs. (3), (6), or (7). Employing Eq. (3) for fluid velocity, Eq. (2) becomes

$$\frac{\rho_c}{\rho} \frac{\partial p}{\partial r} + \left(\frac{R}{r} \right)^2 \ddot{R} + \frac{2}{r} \left(\frac{R}{r} \right) \dot{R}^2 \left(1 - \left(\frac{R}{r} \right)^3 \right) = 0 \quad (8)$$

Eq. (8) later will be useful in determining the maximum pressure gradient $\frac{\partial p}{\partial r}$, and hence, the maximum acceleration load. In order to obtain $R(t)$, $\dot{R}(t)$, and $\ddot{R}(t)$ for a submerged bubble, we may employ the conditions that bubble pressure P_B is exerted on the fluid at radius R , and

for these conditions, we obtain the classic Rayleigh bubble equation,

$$R \ddot{R} + \frac{3}{2} \dot{R}^2 = \frac{g_c}{\rho} (P_B - P_\infty) \quad (9)$$

A solution to Eq. (9) will provide $R(t)$, $\dot{R}(t)$, and $\ddot{R}(t)$ for use in Eqs. (3), (6), or (7) to specify properties of the flow field.

STEADY DRAG FORCE

When an object is submerged in a fluid whose bulk steady flow velocity is U_∞ , the steady drag force is calculated by an equation of the form,

$$F_{\text{STAN}} = C_D A \frac{U_\infty^2}{2g_c} \rho \quad (10)$$

where ρ is fluid density, A is the projected area of the object on a plane normal to the direction of flow, and C_D is a drag coefficient. An appropriate velocity for use in Eq. (10) would be determined from Eq. (6) for a flow field generated by a spherical bubble.

Sometimes it is necessary to predict steady pressure and skin friction drag forces separately, utilizing tables or graphs for C_D found in most basic fluid mechanics textbooks, (e.g., Binder, 1956, or Olsen, 1973). However, the nature of such drag forces during unsteady flow must be examined to determine if the steady drag forces are adequate for design considerations.

Pressure drag on a submerged object is based on the sum of all incremental pressure forces around its surface. It is well known that in classical inviscid flow theory, no boundary layer separation or downstream wakes occur during flow past a submerged object, and the net ideal pressure drag is zero. However, boundary layer separation and resulting turbulent wakes behind a submerged object occur in most real flows and provide the mechanism for pressure drag.

When fluid is accelerated from rest past an object, or when an object is accelerated into stationary fluid, it has been determined that the early flow resembles that of inviscid fluid without separation (Schlichting, 1955). Therefore, during the flow accelerations associated with unsteady flows, pressure drag forces will be less than the final steady state value. It follows that steady flow predictions will provide an upper limit for pressure drag forces.

Pressure drag forces

TIME-DEPENDENT SKIN FRICTION DRAG

Drag due to skin friction is the result of viscous shear stress on the surface of an object. Shear stress is obtained from the defining equation,

$$\tau = \mu \frac{\partial u}{\partial y}$$

(11)

where μ is the dynamic viscosity, u is the bulk fluid velocity component parallel to the surface determined from

Eq. (6) for gas-bubble flows, and y is distance normal to the surface. Behavior of the skin friction drag during accelerating flow across a surface can be determined from the simplified analysis described in Fig. 1. The initial

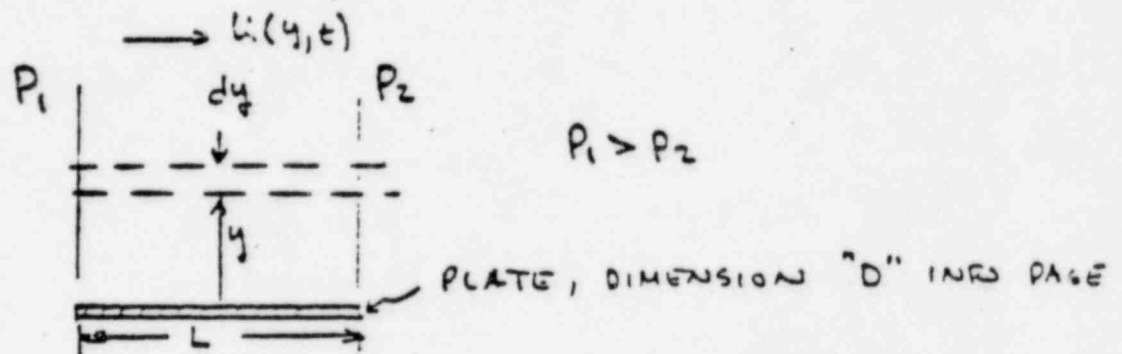


Figure 1 Unsteady Skin Friction Drag Determination

fluid velocity $u(y,0)$ is taken as zero. Pressures P_1 and P_2 suddenly are applied at each end of the plate whose length is L and whose depth into the page is D . Since there are no vertical forces, parallel left-to-right fluid motion will occur. Resulting wall shear τ is obtained from Eq. (11) with $\frac{\partial u}{\partial y}$ evaluated at $y=0$. When motion begins, liquid in contact with the plate will be at zero velocity and far from the plate, the shear will be zero. Momentum conservation for a horizontal fluid strip of vertical thickness dy and area DL parallel to the plate leads to a differential equation which governs the flow behavior. The full problem is specified as

$$DE \quad \frac{\partial u}{\partial t} - \nu \frac{\partial^2 u}{\partial y^2} = \frac{g_c}{g} \frac{(P_1 - P_2)}{L} \quad (12)$$

$$IC \quad u(y,0) = 0 \quad (13)$$

$$BC \quad u(0,t) = 0 \quad (14)$$

$$\tau(\infty,t) = \frac{\partial u}{\partial y}(\infty,t) = 0 \quad (15)$$

the velocity $u(y, t)$ is given by

$$u(y, t) = \frac{q_c}{\rho} \frac{(P_1 - P_2)}{L} t \left(1 - \frac{4}{\pi} \int_0^{\frac{y}{2\sqrt{\nu t}}} \left(\xi - \frac{y}{2\sqrt{\nu t}} \right)^2 e^{-\xi^2} d\xi \right) \quad (16)$$

Applying rules for differentiating integrals, it follows that shear stress at the plate is

$$\tau_w = \tau(0, t) = \mu \frac{\partial u}{\partial y}(0, t) = 2 \frac{(P_1 - P_2)}{L} \sqrt{\frac{\nu t}{\pi}} \quad (17)$$

and the total skin friction drag on one side is

$$F = \tau_w DL = 2 (P_1 - P_2) D \sqrt{\frac{\nu t}{\pi}} \quad (18)$$

Eq. (18) shows that skin friction drag starts at zero and increases during flow acceleration. When steady flow is reached in any fluid of finite extent, the skin friction drag will have reached its maximum value. It follows that steady flow predictions will provide maximum values of skin friction drag forces on submerged objects.

What are the steady flow conditions?

MAXIMUM PRESSURE GRADIENT AND ACCELERATION DRAG

Pressure and skin friction drag forces depend on local velocity, which is seen to be proportional to bubble wall velocity \dot{R} in Eq. (6). When $\dot{R} = 0$, these drag forces are zero. However, Eq. (8) shows that even if $\dot{R} = 0$, a pressure gradient $\frac{\partial P}{\partial r}$ can occur if bubble wall acceleration $\ddot{R} \neq 0$. Resulting acceleration drag forces on submerged structures will be considered next. Substituting \ddot{R} from Eq. (9) into Eq. (8), the pressure gradient is given by

$$\frac{d}{dt} \left[\frac{4}{3} \pi r^3 \rho \left(\frac{P_0 - P_0}{\rho} - \frac{2}{3} R^2 \right) \right] - \frac{2}{r} \left(\frac{P_0}{\rho} \right) R^2 \left(1 - \left(\frac{R}{r} \right)^2 \right) = 0$$

During air charging, a submerged bubble will expand. When air charging stops, the bubble will undergo oscillatory motion. It is necessary to consider the pressure gradient behavior during both charging and oscillatory motions to determine maximum acceleration loads. First, the bubble motion will be examined.

Eq. (9) describes bubble motion for a given bubble pressure P_B . In order to determine bubble motion, another relationship for bubble pressure is required, which is obtained from mass and energy conservation. Figure 2 shows a bubble

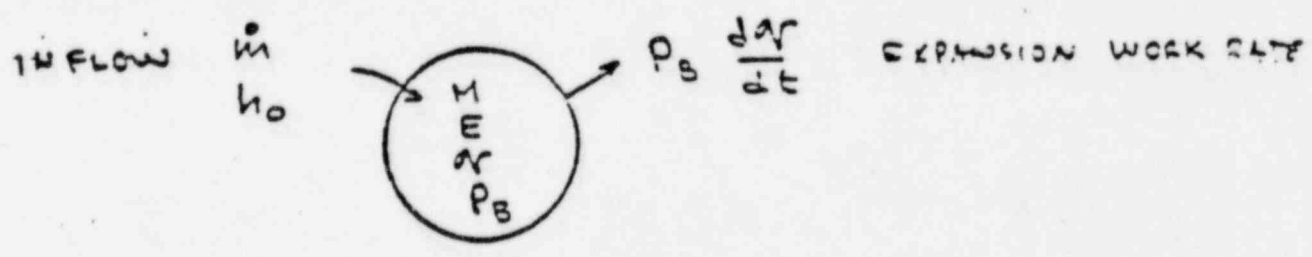


Figure 2 Bubble Mass and Energy Conservation

being charged by mass flow rate \dot{m} and incoming stagnation enthalpy h_0 . Energy leaves the bubble by expansion work on the surroundings, and heat transfer effects are neglected. It follows that

MASS $\dot{m} = \frac{dM}{dt}$

ENERGY $P_B \frac{dV}{dt} - \dot{m} h_0 + \frac{dE}{dt} = 0$

Employing the state equations

$$h_0 = \frac{\gamma}{\gamma-1} \frac{P_0}{\rho_0} \quad , \quad E = \frac{1}{\gamma-1} P_2 V$$

and expressing the volume of a spherical bubble as

$$V = \frac{4}{3} \pi R^3$$

we obtain the equation

$$\frac{dP_B}{dt} = \frac{3\gamma}{4\pi R^2} \frac{P_0}{\rho_0} \dot{m} - 3\gamma \frac{P_B}{R} \dot{R} \quad (20)$$

which relates bubble pressure rate with wall velocity and charging properties. In order to find the maximum pressure gradient, Eq. (19) is differentiated with respect to time to obtain its rate of change at arbitrary distance r . Since $\frac{q_c}{\rho} \frac{\partial P}{\partial r}$ is negative in most regions of interest when $P_3 - P_\infty > 0$, if it can be shown that $\frac{\partial}{\partial t} \left(\frac{\partial P}{\partial r} \right) > 0$, we may conclude that the negative pressure gradient is becoming less negative, and acceleration loads are decreasing. Therefore, information on the rate of change of pressure gradient will be useful in determining conditions for maximum acceleration loads. When Eq. (19) is differentiated with respect to time, and Eqs. (9) and (20) are employed to eliminate \ddot{R} and \dot{P}_B , we obtain

$$r^2 \frac{\partial}{\partial t} \left(\frac{q_c}{\rho} \frac{\partial P}{\partial r} \right) = \frac{q_c}{\rho} P_3 \dot{R} \left(3\gamma - 2 + 4 \left(\frac{R}{r} \right)^3 \right) + \frac{q_c}{\rho} P_\infty \dot{R} \left(2 - 4 \left(\frac{R}{r} \right)^3 \right) + \dot{R}^3 \left(1 + 2 \left(\frac{R}{r} \right)^3 \right) - 3\gamma \frac{q_c}{\rho} \frac{1}{4\pi R^2} \frac{P_0}{\rho_0} \dot{m} \quad (21)$$

Several observations can be made immediately from Eqs. (19) and (21) :

Observation 1 Maximum pressure gradient for an oscillating bubble occurs simultaneously with zero bubble wall velocity.

For the case $\dot{m}=0$ after bubble charging is complete and during oscillating motion, the pressure gradient at any r reaches either a maximum or minimum when $\dot{R}=0$, which occurs simultaneously with either maximum or minimum bubble radius, or

$$\frac{\partial P}{\partial r} \Big|_{MAX} = -\frac{R}{r^2} (P_B - P_\infty) ; \quad (22)$$

The value of $R(P_B - P_\infty)$ employed should be either $R_{MIN}(P_{BMAX} - P_\infty)$ or $R_{MAX}(P_{BMIN} - P_\infty)$, whichever has the largest absolute value.

Observation 2 The pressure gradient becomes less steep after charging stops. At the instant charging stops, that is, when

\dot{m} suddenly becomes zero, we have $\dot{R} > 0$ for which the pressure gradient will become less negative ($\frac{\partial}{\partial t} \left(\frac{\partial P}{\partial r} \right) > 0$), and acceleration loads will decrease, as long as $P_B - P_\infty > 0$.

This conclusion is reached by first writing Eq. (21) as

$$r^2 \frac{\partial}{\partial t} \left(\frac{\partial P}{\partial r} \right) = \frac{4\gamma}{3} \dot{R} P_B (3\gamma - 2) + \frac{29\gamma}{3} P_\infty \dot{R} + 4 \left(\frac{R}{r} \right)^3 \frac{4\gamma}{3} \dot{R} (P_B - P_\infty) + (1 + 2 \left(\frac{R}{r} \right)^3) \dot{R}^3$$

The pressure gradient $\frac{\partial P}{\partial r}$ is negative for $\frac{R}{r} < \left(\frac{1}{4} \right)^{1/3}$, and noting that all terms on the right are greater than zero for

$\gamma = 1.4$, $\dot{R} > 0$, and $P_B - P_\infty > 0$, the conclusion is valid.

Observation 3 During bubble charging, the pressure gradient may increase or decrease with time. During bubble charging, it is difficult to tell from Eq. (21) whether $\frac{\partial P}{\partial r}$ becomes more or less steep with time. Initially if the bubble mass charging rate and volume expansion rate are related by

$$\dot{m} = \rho_0 4\pi R^2 \dot{R}$$

and $P_B = P_0$, the pressure gradient becomes

$$r^2 \frac{\partial}{\partial t} \left(\frac{\rho_c}{3} \frac{\partial P}{\partial r} \right) \Big|_{t=0} = \dot{R} \left[-\frac{\rho_c}{3} \left(2 - 4 \left(\frac{R}{r} \right)^3 \right) (P_0 - P_\infty) + \dot{R}^2 \left(1 + 2 \left(\frac{R}{r} \right)^3 \right) \right]$$

Unfortunately, the right hand side can be either positive or negative, depending on the magnitudes of P_0 and \dot{R} .

Since the pressure gradient can be increasing or decreasing during charging as shown from observation 3, we will attempt to find an upper limit value of $\frac{\partial P}{\partial r}$ from Eq. (19) for the case $P_B - P_\infty > 0$. Note that if \dot{R}^2 is a maximum value, the two terms $-\frac{\rho_c}{3} (P_0 - P_\infty)$ and $-\frac{\dot{R}^2}{2}$ will add whenever $\frac{R}{r} < \left(\frac{1}{4}\right)^{\frac{1}{3}}$. For submerged structures inside this region, the two terms will subtract, yielding lower acceleration loads. Therefore, a case in which these two terms are largest will correspond to the maximum $\frac{\partial P}{\partial r}$. In order to determine the maximum \dot{R} , we rewrite Eq. (9) as

$$R \frac{d\dot{R}}{dt} = \frac{\rho_c}{3} (P_B - P_\infty) - \frac{3}{2} \dot{R}^2$$

from which it is noted that the maximum \dot{R} at any P_B corresponds to

$$\dot{R}^2 = \frac{2}{3} \frac{\rho_c}{3} (P_B - P_\infty) \quad (23)$$

The maximum value of P_B generally occurs just as bubble charging begins, and subsequently decreases if drywell pressure decreases when venting begins, and since expansion of the initially forming spherical bubble reduces bubble pressure.

Then, substituting for the air charging rate

$$\dot{M} = 3a 4\pi R^2 \dot{R} \quad (24)$$

Eq. (20) becomes for $P_B = P_{B,MAX} = \text{CONST}$,

$$\frac{dP_B}{dt} = \frac{\gamma}{R} \left(\frac{\rho_a}{\rho_0} P_0 - P_{BMAX} \right) \dot{R} \quad (25)$$

The maximum value of P_B would correspond to $\frac{dP_B}{dt} = 0$, for which we conclude from Eq. (25) that

$$\left. \begin{aligned} \rho_a &= \rho_0 \\ P_{BMAX} &= P_0 \end{aligned} \right\} \quad (26)$$

and

where P_0 and ρ_0 are air properties either in the drywell or in the relief line discharge plane during charging. If \dot{R} from Eq. (23) is used in Eq. (19), it follows that the upper limit value of $\frac{\partial P}{\partial r}$ during charging is

$$\left. \frac{\partial P}{\partial r} \right|_{\text{MAX, CHARGING}} \leq -\frac{4}{3} \frac{R}{r^2} (P_0 - P_a) \quad (27)$$

whereas if the bubble wall velocity term of Eq. (19) is neglected, we have

$$\frac{\partial P}{\partial r} = -\frac{2}{r^2} (P_B - P_a) \quad (28)$$

It follows that including the velocity term in Eq. (19) during charging increases the pressure gradient by only 30 percent. Therefore, it is conservative to obtain the acceleration drag for the pressure gradient of Eq. (27) during bubble charging. If Eq. (23) is integrated from a bubble radius R_0 at $t=0$, we obtain the maximum possible radius at any time t as

$$R = R_0 + \sqrt{\frac{2}{3} \frac{g_c}{g} (P_0 - P_a)} t \quad (29)$$

Now we are in a position to express the uniform flow field acceleration associated with the maximum pressure gradient. Substituting \dot{R} from Eq. (9) into Eq. (7), we obtain

$$\ddot{u}_p(t) = \frac{R(t)}{r^2} \left[\frac{g_c}{g} (P_B - P_a) + \frac{1}{2} \dot{R}^2 \right] \quad (30)$$

For the case of an oscillating bubble, it was shown that

$\dot{R} = 0$ at the maximum pressure gradient of Eq. (22) so that maximum acceleration drag will correspond to either of the relationships,

$$\dot{u}_D(t)|_{MAX} = \frac{1}{r^2} \frac{q_c}{S} \left\{ \begin{array}{l} R_{MIN} (P_{BMAX} - P_\infty) \\ R_{MAX} (P_{BMIN} - P_\infty) \end{array} \right\} \text{ OSCILLATING} \quad (31)$$

depending on which product in braces has the largest absolute value. For the case of a charging bubble, the maximum pressure gradient of Eq. (27) already contains the maximum effect of bubble wall velocity so that Eq. (30) can be written as

$$\dot{u}_D(t)|_{MAX} = \frac{R(t)}{r^2} \left[\frac{q_c}{S} (P_0 - P_\infty) + \frac{1}{2} \dot{R}^2 \right] \leq \frac{R(t)}{r^2} \frac{4}{3} \frac{q_c}{S} (P_0 - P_\infty) \text{ CHARGING} \quad (32)$$

Eqs. (31) and (32) give uniform flow accelerations which will result in the maximum acceleration drag.

We will consider potential flow fields for several submerged structures. The velocity potential ϕ defined by

$$\vec{v} = \nabla \phi \quad (33)$$

is obtained for given geometries from a solution to Eq. (1). Eq. (2) is integrated to give Bernoulli's equation,

$$\frac{q_c}{S} (P - P_\infty) = - \frac{\partial \phi}{\partial t} - \frac{v^2}{2g_L} \quad (34)$$

The procedure for obtaining maximum acceleration loads is to obtain $\frac{\partial \phi}{\partial t}$ corresponding to the maximum pressure gradient for a given structure, use of Eq. (31) to express pressure on the structure surface, and integration over the structure surface area. For uniform flow past a structure, it is well

established that the term $\frac{v^2}{2\gamma_c}$ in Eq. (34) contributes nothing to the force in a potential flow, unless circulation is present, as it would be for an airfoil shape. However, most structures to be considered in a suppression pool are not shaped like an airfoil, and therefore, $\frac{v^2}{2\gamma_c}$ can be dropped from Eq. (34) when integrating acceleration pressure on the structure surface area.

The potential function for uniform flow parallel to the x axis past a structure is usually expressed in the functional form,

$$\phi = f(U_\infty(t), x, y) = \phi(U_\infty(t), r, \theta) \quad (35)$$

It follows that $\frac{\partial \phi}{\partial t}$ can be obtained as

$$\frac{\partial \phi}{\partial t} = \frac{\partial \phi}{\partial U_\infty(t)} \dot{U}_\infty(t) \quad (36)$$

for use in Eq. (34) to determine pressure anywhere in the flow field, and in particular, on the structural surfaces.

The acceleration drag will be obtained next for several geometries which suggest common submerged structural shapes.

ACCELERATION DRAG, SPHERE IN UNIFORM FLOW

Fig. 3 shows a sphere of radius R_s in a uniform flow of velocity $U_\infty(t)$. The associated velocity potential function (Streeter, 1948) is

$$\phi = U_\infty(t) \left(\frac{R_s^3}{2r} + r \right) \cos \theta \quad (37)$$

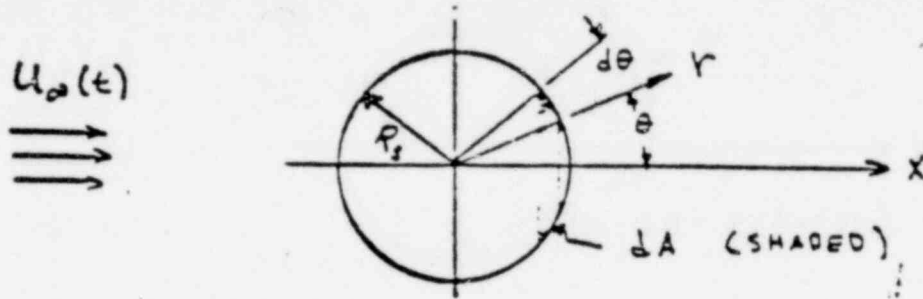


Figure 3 Sphere in Uniform Flow

It follows from Eqs. (34) and (37) with the $\frac{V^2}{2g_c}$ term dropped that pressure on the sphere at conditions of maximum pressure gradient is given by

$$\frac{g_c}{\rho} (P - P_\infty) \Big|_{r=R_s} = - \dot{U}_\infty(t) \frac{3}{2} R_s \cos \theta \quad (38)$$

The incremental surface area indicated in Fig. 3 is

$$dA = 2\pi R_s^2 \sin \theta d\theta$$

Integrating to obtain the maximum acceleration drag force in the direction of the flow, we obtain

$$F = \frac{3}{2} \left(\frac{4}{3} \pi R_s^3 \right) \frac{\rho}{g_c} \dot{U}_\infty(t) \quad (39)$$

where $\dot{U}_\infty(t)$ is determined from Equations (31) or (32).

ACCELERATION DRAG, PIPE IN UNIFORM FLOW

Fig. 4 shows a pipe of radius R_p whose axis is normal

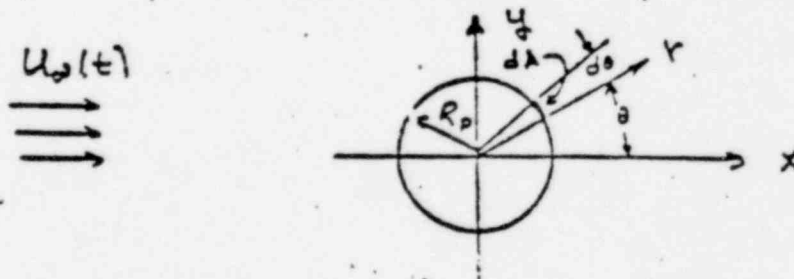


Figure 4 Pipe in Uniform Flow

to a uniform flow, and whose length is L . The classical velocity potential function for this geometry is given by

$$\phi = U_p(t) r \cos \theta \left(1 + \frac{R_p^2}{r^2} \right) \quad (40)$$

It follows from Eqs. (34) and (40) with the $\frac{v^2}{2g_c}$ term dropped that pressure on the pipe at conditions of maximum pressure gradient is given by

$$\frac{g_c}{\rho} (P - P_\infty) \Big|_{r=R_p} = -2 \dot{U}_p(t) R_p \cos \theta \quad (41)$$

The incremental surface area shown in Fig. 4 is

$$dA = R_p L d\theta \quad (42)$$

Integrating the pressure force to obtain the maximum acceleration drag force in the x direction, we obtain

$$F = 2(\pi R_p^2 L) \frac{\rho}{g_c} \dot{U}_p(t) \quad (43)$$

where the term $\dot{U}_p(t)$ is determined from Eqs. (31) or (32).

ACCELERATION DRAG, PLATE IN UNIFORM FLOW

Fig. 5 shows a thin plate of width H and length L into

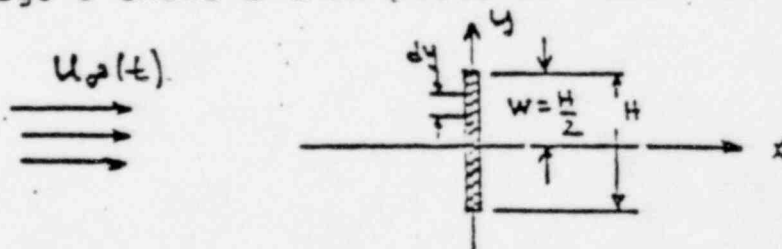


Figure 5 Thin Plate in Uniform Flow

the page, facing in the direction of a uniform flow. The velocity potential function for the geometry of Fig. 5 is given in the form (Vallentine, 1959),

$$\phi^2 - \frac{u_\infty(t)^4 x^2 y^2}{\phi^2} = u_\infty^2(t) (x^2 - y^2 + w^2) \quad (44)$$

At $x=0$, $y \neq 0$ we have

$$\phi = \pm u_\infty(t) \sqrt{w^2 - y^2}$$

and Eq. (34) provides the pressure on the plate as

$$\frac{\rho}{2} (P - P_\infty) = \pm \dot{u}_\infty(t) \sqrt{w^2 - y^2} \quad (45)$$

where the double sign refers to left and right sides respectively. Using an area element

$$dA = L dy \quad (46)$$

the net acceleration force obtained by integrating on both sides is

$$F = \frac{1}{4} (\pi H^2 L) \frac{\rho}{g_c} \dot{u}_\infty(t) \quad (47)$$

where again $\dot{u}_\infty(t)$ is determined from Eqs. (31) or (32).

ESTIMATED ACCELERATION DRAG FOR OTHER STRUCTURES

Analytical solutions have been employed for a sphere, pipe, and flat plate in a uniform flow field. However, angles with L-shaped cross sections and I-beams are common submerged structural members for which analytical solutions are not readily available if at all. Therefore, it is

desirable to estimate the acceleration drag on angles and I-beams.

If one side of an angle is oriented in the direction of a uniform flow, we have the situation shown in Fig. 6(a).

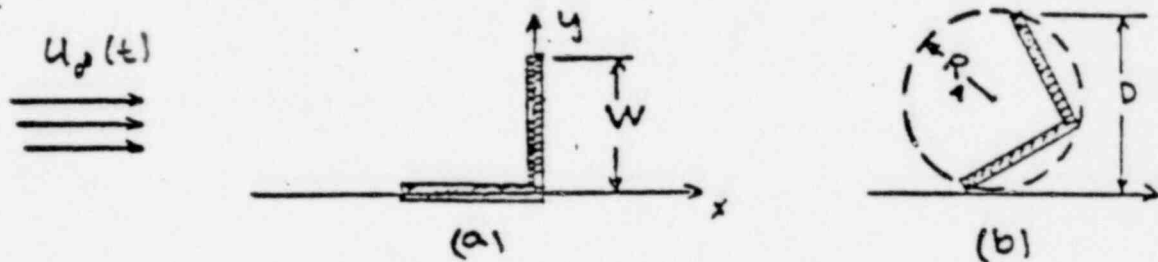


Figure 6 Angle in Uniform Flow

Since the associated flow pattern corresponds to the top half of the symmetric flow pattern of a flat plate shown in Fig. 5, the acceleration drag force can be expressed as

$$F = \frac{1}{2} (\pi W^2 L) \frac{\rho}{q_c} \dot{U}_p(t) \quad (48)$$

However, if the angle is oriented some other way as suggested in Fig. 6(b), the effect on acceleration drag is not obvious. The geometry might be treated as another flat plate of width D equal to the maximum dimension normal to the flow field, which for equally wide sides would result in a maximum drag obtained from Eq. (47) as

$$F = \frac{1}{4} (\pi D^2 L) \frac{\rho}{q_c} \dot{U}_p(t) = \frac{\pi W^2 L}{2} \frac{\rho}{q_c} \dot{U}_p(t) \quad (49)$$

which is the same as Eq. (48). Another bounding calculation corresponds to the acceleration drag on a circumscribed

equivalent pipe shown dotted in Fig. 6(b), for which Eq. (43) gives

$$F = 2 (\pi R_A^2 L) \frac{\rho}{q_c} \dot{U}_\infty = (\pi w^2 L) \frac{\rho}{q_c} \dot{U}_\infty \quad (50)$$

Comparing Eqs. (48), (49), and (50), it is clear that Eq. (50) gives the highest acceleration drag, and is preferred for conservative estimates.

An I-beam also may have various orientations in a uniform flow field. Since the circumscribed pipe gave highest acceleration drag for an angle, the same method is used to estimate acceleration drag for a submerged I-beam, where R_s in Eq. (43) is the circumscribed radius, R_I .

VALID RANGE OF PRESENT ANALYSIS

Eqs. (39), (43), and (47) give acceleration drag forces proportional to the free stream acceleration, $\dot{U}_\infty(t)$.

Eqs. (32) or (31) give \dot{U}_∞ in the form

$$\dot{U}_\infty = \frac{c}{r^2} \frac{q_c}{S} R (\rho_B - \rho_\infty) \quad (51)$$

where c is 1.0 for bubble oscillation or 4/3 for bubble charging. However, there may be a limit on how small r can be for a valid prediction of acceleration drag. This limitation will be considered next.

Pressure exerted on a submerged object by oscillating bubbles will not exceed that of the bubbles at extremes in oscillation when $\dot{R} = 0$. This can be proved by operating on Eq. (34) with ∇^2 when $V=c$, which leads to

$$\frac{1}{\rho} \nabla^2 p = - \frac{\partial}{\partial t} \nabla \cdot \mathbf{v} \quad (52)$$

Since Eqs. (1) and (33) show that ϕ satisfies $\nabla^2 \phi = 0$, it follows from Eq. (52) that

$$\nabla^2 p = 0 \quad \text{when } \mathbf{v} = 0 \quad (53)$$

Eq. (53) has the same form as the steady heat conduction equation, $\nabla^2 T = 0$, for which it is well established that no temperature in a closed region or on a non-flow (insulated) part of the boundary can exceed the highest temperature which occurs elsewhere on the boundary. Extending this characteristic to Eq. (53), it follows that pressure on any non-flow boundary cannot exceed pressure occurring in the bubble. It is expected that the same conclusion is valid even when the flow field velocity is not zero, since the bubble is free to distort or to move away from a submerged boundary.

Based on the limitation that pressure on a submerged object may not exceed that of the bubble, we will substitute Eq. (51) into the surface pressure equations for a sphere, pipe, and plate, and require that the stagnation point pressure be less than or equal to bubble pressure. This procedure will establish limits on r .

For a sphere in a uniform flow, we have from Eqs. (38) and (51) at the stagnation point $\theta = \pi$,

$$\frac{R_0 R}{r^2} \leq \frac{2}{3} \frac{1}{c} \quad \text{SPHERE} \quad (54)$$

For a pipe in a uniform flow, we have from Eqs. (41) and (51) at the stagnation point $\theta = \pi$,

$$\frac{R_0 R}{r^2} \leq \frac{1}{2c} \quad \text{PIPE} \quad (55)$$

For a plate in uniform flow, we have from Eqs. (45) and (51) at the stagnation point $y=0$,

$$\frac{HR}{r^2} \leq \frac{2}{C} \quad \text{PLATE} \quad (56)$$

Eqs. (54), (55), and (56) give the range of validity for r in terms of bubble size and a characteristic dimension of the submerged structure so that no pressure on the surface of a structure exceeds bubble pressure. In each case, both bubble radius R and the characteristic size of the submerged object must be less than r , leading to the further constraint,

$$\left. \begin{aligned} \frac{R}{r} < 1 \\ \frac{R_s}{r} < 1, \quad \frac{R_p}{r} < 1, \quad \frac{H}{r} < 1 \end{aligned} \right\} \quad (57)$$

ESTIMATE OF TOTAL DRAG ON SUBMERGED STRUCTURES

Total fluid force on a submerged structure is approximated as the sum of both acceleration and standard drag,

$$F_{\text{TOTAL}} = F_{\text{ACCEL}} + F_{\text{STAN}} \quad (58)$$

where F_{ACCEL} and F_{STAN} are based on instantaneous flow properties. We may use Eq. (10) for the standard drag force associated with a uniform flow velocity U_∞ once the steady flow pressure and skin friction drag coefficients are obtained for the particular submerged structure. Although the expressions for acceleration drag are for the maximum value, the uniform flow acceleration $\dot{U}_\infty(t)$ will be considered the instantaneous value for acceleration drag forces other than

maximum. For all the submerged structures considered, the acceleration drag is written in the form

$$F_{ACCEL} = K \frac{\rho}{g_c} \dot{U}_\infty(t) \quad (59)$$

where from Eqs. (39), (43), (47), and (50) the constant K takes on values,

$$\left. \begin{aligned} K_{SPHERE} &= \frac{3}{2} \left(\frac{4}{3} \pi R_S^3 \right) & K_{ANGLE} &= 2 (\pi R_A^2 L) \\ K_{PIPE} &= 2 (\pi R_P^2 L) & K_{I-BEAM} &= 2 (\pi R_I^2 L) \\ K_{PLATE} &= \frac{1}{4} (\pi H^2 L) \end{aligned} \right\} \quad (60)$$

Using Eqs. (6) and (7) for $U_\infty(t)$ and $\dot{U}_\infty(t)$, Eq. (58) gives the total drag as

$$F_{TOTAL} = \frac{\rho}{g_c} \left\{ K \left[\ddot{R} \frac{R^2}{r^2} + \frac{2}{r^2} R \dot{R}^2 \right] + \left(\frac{C_{DA}}{2} \right) \dot{R}^2 \left(\frac{R}{r} \right)^4 \right\} \quad (61)$$

For a charging bubble, Eqs. (61) and (23) give

$$F_{TOTAL} = \frac{\rho}{g_c} \dot{R}^2 \left(\frac{R}{r} \right)^2 \left[2 \frac{K}{R} + \left(\frac{C_{DA}}{2} \right) \left(\frac{R}{r} \right)^2 \right] \quad \text{CHARGING} \quad (62)$$

and for an oscillating bubble, Eqs. (9) and (61) give

$$F_{TOTAL} = \frac{\rho}{g_c} \left\{ \frac{K R}{r^2} \left[\frac{4}{3} (\rho_B - \rho_\infty) + \frac{1}{2} \dot{R}^2 \right] + \left(\frac{C_{DA}}{2} \right) \dot{R}^2 \left(\frac{R}{r} \right)^4 \right\} \quad \text{OSCILLATING} \quad (63)$$

EXAMPLE: COMPUTATION, SUBMERGED PIPE

Eqs. (23), (60), (62), and (63) and the projected area $A = 2 R_P L$ give the total drag force on a submerged pipe as

$$\frac{F_{TOTAL}}{(P_B - P_\infty)A} \Big|_{CHARGING} = \frac{4}{3} \pi \frac{R_0 R}{r^2} + \frac{C_D}{3} \left(\frac{R}{r}\right)^4 ; \quad \left\{ \begin{array}{l} \frac{R_0 R}{r^2} \leq \frac{3}{8} \\ \frac{R}{r} \leq 1 \\ \frac{R_0}{r} \leq 1 \end{array} \right\}$$

and

$$\frac{F_{TOTAL}}{P_\infty A} \Big|_{OSCILLATING} = \pi \frac{R_0 R}{r^2} \left[\left(\frac{P_B}{P_\infty} - 1 \right) + \frac{\dot{R}^2}{(2.9 C_D P_\infty)} \right] + \frac{\dot{R}^2}{(2.9 C_D P_\infty)} C_D \left(\frac{R}{r}\right)^4 \quad \left\{ \begin{array}{l} \frac{R_0 R}{r^2} \leq \frac{1}{2} \\ \frac{R}{r} \leq 1 \\ \frac{R_0}{r} \leq 1 \end{array} \right\}$$

Computations were done for a submerged pipe with $R_p = 1.0$ ft a distance $r = 10$ ft from the bubble center, and a drag coefficient $C_D \approx 1.0$. Figs. 7 and 8 show resulting total drag forces in terms of bubble radius. The oscillating case was based on a computation for which $\frac{P_{BMAX}}{P_\infty} = 18.3$ at $R = R_{MIN}$, and the bubble radius at P_∞ corresponding to $R_\infty = 2R_{MIN}$.

Both acceleration and standard drag components are seen to increase as R increases in Fig. 7 for the charging bubble example. This suggests that the drag force specified for design should be that value at maximum bubble radius. In the oscillating bubble case of Fig. 8, maximum total drag occurs at minimum bubble radius, and decreases with bubble expansion.

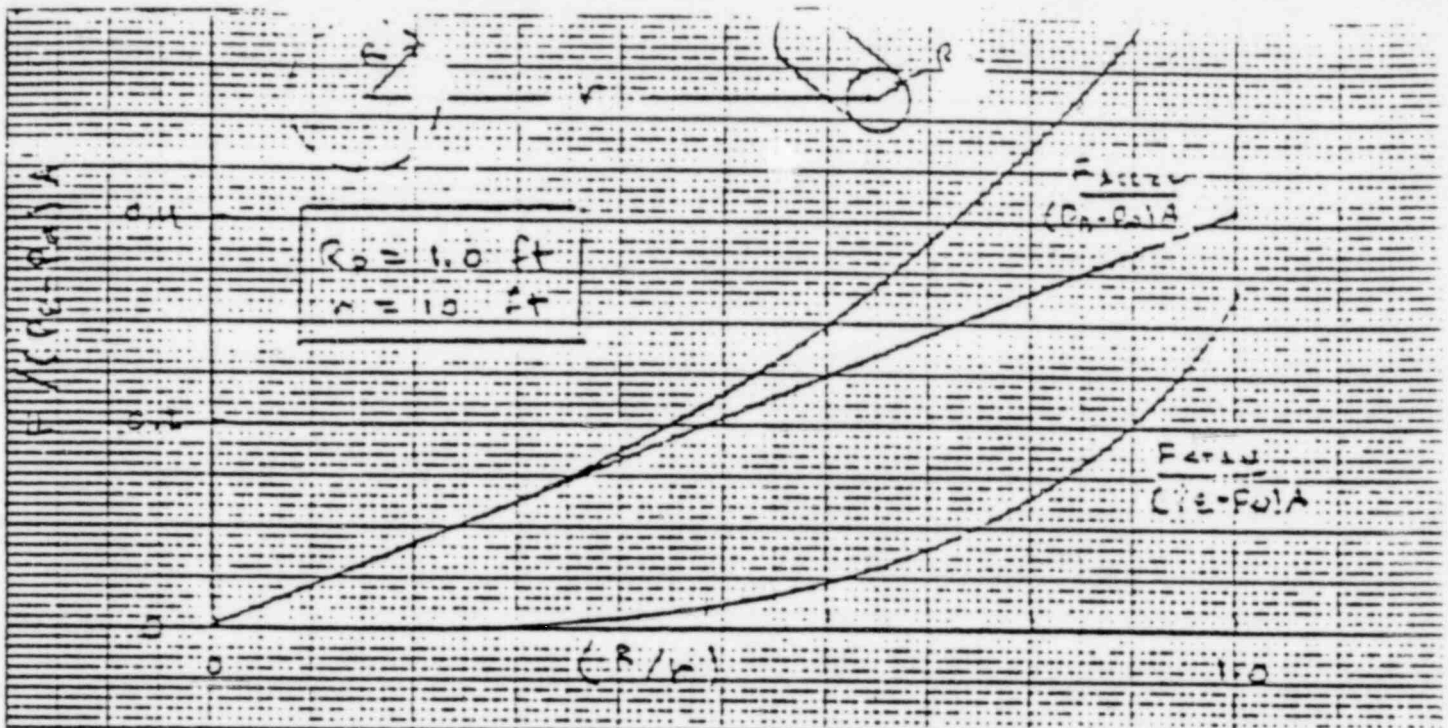


FIGURE 7. EXAMPLE CHARGING BUBBLE DRAG FORCES

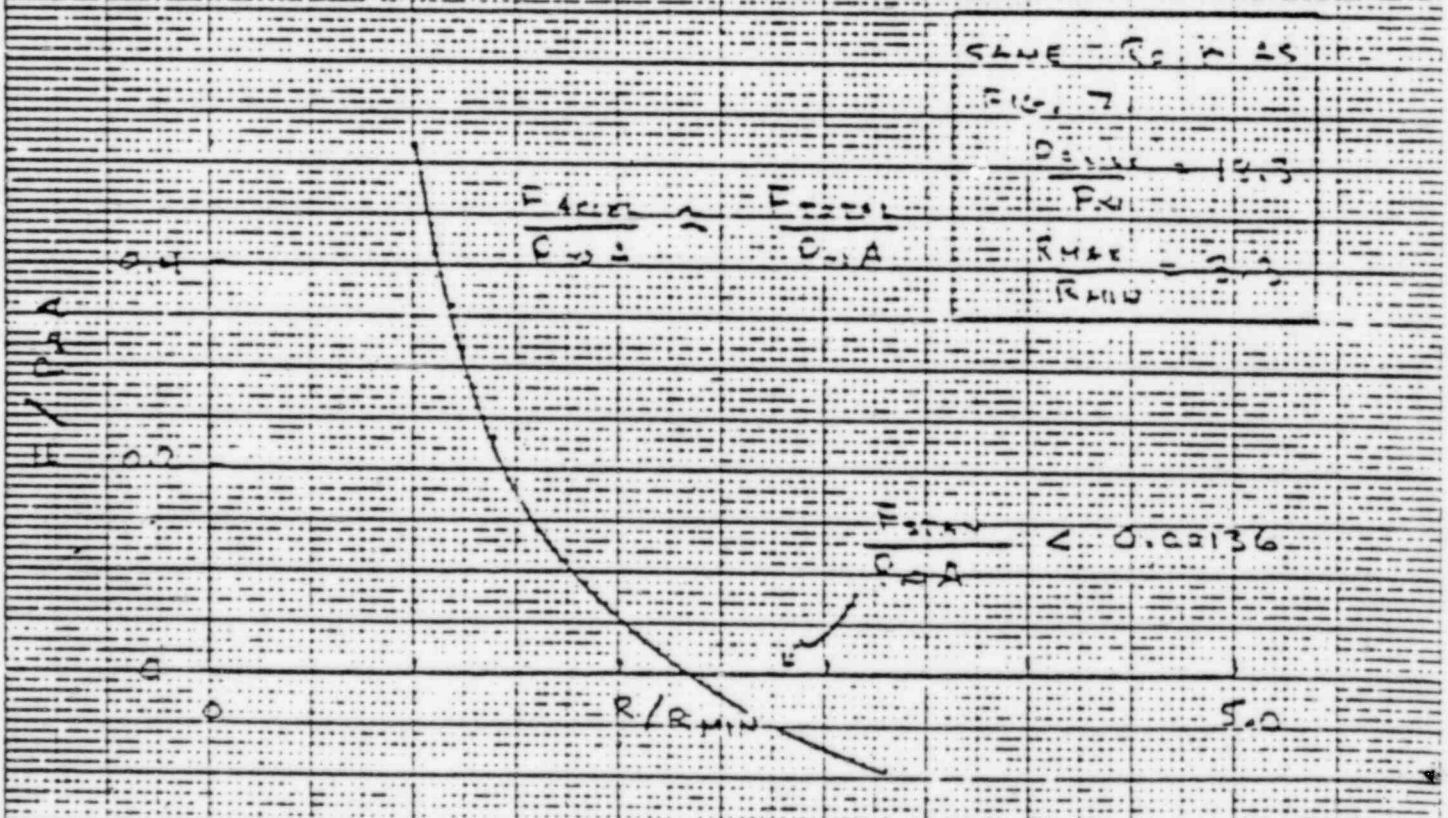


FIGURE 8. EXAMPLE OSCILLATING BUBBLE DRAG FORCES

REFERENCES

- Binder, R. C., Fluid Mechanics, Prentice-Hall, 1955
- Olsen, R. M., Essentials of Engineering Fluid Mechanics,
Intext, 1973
- Schlichting, H., Boundary Layer Theory, Pergamon, 1955
- Streeter, V. L., Fluid Dynamics, McGraw-Hill, 1948
- Vallentine, Applied Hydrodynamics, London-Butterworth,
1959